ELSEVIER

Polymer 42 (2001) 5479–5484

polymer

www.elsevier.nl/locate/polymer

Stratification processes in thermoplastic olefins monitored by step-scan photoacoustic FT-IR spectroscopy

J.M. Stegge, M.W. Urban*

Shelby F. Thames Polymer Science Research Center, School of Polymers and High Performance Materials, University of Southern Mississippi, Box 10076, Hattiesburg, MS 39406-0076, USA

Received 16 April 2000; received in revised form 29 October 2000; accepted 1 November 2000

Abstract

In this study we utilized step-scan photoacoustic Fourier transform IR (SS-PA-FT-IR) spectroscopy to examine surface/interfacial properties of thermoplastic olefins (TPOs). This approach, combined with 2D FT-IR correlation analysis, allowed us to determine stratification processes in TPOs. These studies showed that the talc and polypropylene (PP) crystalline phase in TPO stratifies within the first 6–30 μm from the surface. Specifically, the PP crystalline phase exists at about 6.5 μm from the surface and its content diminishes at 7.1 μm, followed by reappearance around 11.3 μm, and becomes more prevalent upon approaching the bulk of TPO. Talc concentration levels show a similar pattern of change with depth across the interface, although absolute concentration levels differ from those of crystalline PP. These studies also demonstrated that SS-PA-FT-IR is a powerful tool in surface analysis, in particular for surface/interfacial analysis of multi-component polymeric systems.

Keywords: Stratification process; Thermoplastic olefins; Step-scan photoacoustic FT-IR spectroscopy

1. Introduction

Thermoplastic olefins (TPOs) are composite organic/inorganic systems that consist of a number of components, such as polypropylene (PP) with its various crystalline forms, ethylene–propylene rubber (EPR) and ethylene–butylene rubber (EBR) elastomers, and talc ($Mg(OH)_2$-Si_4O_{10}). Because injection molding is a common manufacturing process used in the production of TPOs, thermal and shear gradients may result in component stratification, thus resulting in different surface and interfacial properties [1–3]. Previous depth profiling studies [4] utilizing continuous scan photoacoustic FT-IR (PA-FT-IR) spectroscopy showed that talc is preferentially located at 5–7 μm below the surface, while crystalline PP is detected at 7–9 μm depths. On the other hand, an EPR layer was detected at 15 μm from the surface and extends into the bulk PP. This elastomer rich region corresponds to the area, in the current experiments, with a PP crystalline phase and talc depletion. Recently, the utility of step-scan PA (SS-PA) analysis for sample stratification has also been demonstrated [5]. Although these studies established the fact that PA-FT-IR spectroscopy can be effectively used in the analysis of multi-component systems, further understanding of stratification processes is necessary in order to relate usually small molecular level changes with significant macroscopic properties.

For that reason we expand the scope of the previous studies and utilize phase analysis [5] in PA-FT-IR surface depth profiling experiments. The majority of methods used for analysis of multi-component systems, such as TPO, are destructive. The technique that offers non-destructive features and allows probing surfaces on a molecular level is step-scan photoacoustic Fourier transform IR (SS-PA-FT-IR) spectroscopy. SS-PA-FT-IR experiments can be utilized to collect information from selectable and constant depths from the sample surface, but limitations may arise due to interference of signals from sample areas above the desired sampling depth. In order for the signal to be produced, heat generated within the first thermal diffusion length should travel through the sample from the depth of origin to the surface. Phase rotational analysis [6–9] attempts to minimize or overcome these limitations. Furthermore, it is beneficial to spread the spectral information over another dimension, which can be accomplished by introducing time dependence to the signal detection, and monitoring the sample response to perturbations. While various external perturbations, including mechanical, heat, and magnetic field variations, have been employed to induce time

* Corresponding author. Tel.: +1-601-266-6454; fax: +1-601-266-5635.
E-mail address: marek.urban@usm.edu (M.W. Urban).

0032-3861/01/$ - see front matter
PII: S0032-3861(00)00852-1

dependence into a system [6,10–14], photothermal internal perturbations have been employed without the realization that this is an internal perturbation [6,15,16]. Although Jiang et al. [17] pointed out that this analysis can utilize PA amplitude and phase correlations, the mechanism describing this type of perturbation and two-dimensional aspects used to enhance spatial resolution to determine stratification and interactions among surface components were not addressed. Our goal is to take advantage of the fact that photothermal effects in PA-FT-IR detection generate internal perturbations and apply this approach to determine stratification and interactions among TPO components.

2. Experimental

Compounded TPO specimens were obtained from Ford Motor Company as 3.8 mm thick injection molded plaques. PA-FT-IR spectra were recorded using a Bruker Instruments Equinox 55 FT-IR spectrometer in a SS mode and equipped with a MTEC Model 100 PA accessory. Before each data collection, the PA cell was purged with dry He for 5 min. The spectra were collected in the 4000–400 cm^{-1} spectral region, with a spectral resolution of 8 cm^{-1} and double-sided interferograms. Four modulation frequencies, 585, 488, 195, and 22 Hz, were employed to collect data, and spectral phase angle settings were set automatically by the instrument using the instrumentally determined phase angle maximum of a carbon black filled elastomer reference. The necessity of using modulated light comes from the fact that the thermal diffusion length (μ_{th}) is inversely proportional to the square root of modulation frequency (f) and the proportionality constant is thermal diffusivity α [18]. Because $f = 2V\nu$, where V is a speed of a mirror in Michelson interferometer (cm) and ν is the wavenumber (cm^{-1}), μ_{th} is ν dependant. Although this relationship is highly advantageous because by changing f, one can change the distance from which thermal waves can reach the surface, its major drawback is the wavenumber dependence. That is molecular information from, for example, 3000 cm^{-1} will come from shallower surface depths that that from 1000 cm^{-1}. In an effort to overcome this problem SS modes in an interferometric detection can be used, which is accomplished by stopping a mirror at a given retardation point and oscillating it with the frequency f at a given wavenumber. Thus, the Fourier frequency f now is an oscillation frequency, all wavenumbers are modulated at the same Fourier frequency, data collection is continued point-by-point in a SS fashion, and the spectrum is obtained. As a result, f, and therefore μ_{th}, become independent of ν.

It should be pointed out that the conversion of electromagnetic energy to thermal waves in the PA effect may occur not only via thermal de-excitation, which is primarily considered here, but also through luminescence, photochemical and photo-electrical processes, and the energy transfer. In this case the instrument automatically maximizes the signal detected by sequentially examining all phase angles for maximum detector response. This signal represents the surface of this reference material, and the resulting phase angle is directed to the in-phase (I) detector channel and represents strongly absorbing surface signal equal to in-phase (0°) signal. Replacement of the reference with a specimen of interest and collection of two orthogonal signals (0 and 90°) completes the data collection process [17]. Each modulation frequency produces a characteristic instrumental phase value. The number of spectral co-additions needed for a satisfactory signal-to-noise ratio depends on the modulation frequency used for the data collection. In a typical experiment, higher modulation frequencies require longer acquisition times.

In our effort to estimate the depths from which signal is detected it is necessary to know thermal properties of a specimen. In the case of TPO the following values were used for calculations of thermal diffusivity (α): PP thermal conductivity, $\kappa = 0.00135$ W/cm K, density, $\rho = 0.902$ g/cm^3, and specific heat, $C_p = 1.926$ J/g K. The resulting calculated value of α, 7.8×10^{-4} cm^2/s, was used to estimate the penetration which corresponds to photothermal perturbation depth. While Section 3 provides a mathematical description of PA depth of penetration equations, Table 1 correlates modulation frequency and approximate depths of perturbation. It should be noted that this is only an estimate of thermal properties of TPO; however, because PP represents about 70% of the total mixture, and since the EPR/EBR, which is one of the other main components of TPO, exhibits similar thermal properties, this estimate is quite reliable.

Opus software (Bruker Instruments) was used for data manipulation, including 2D FT-IR analysis. All spectra were normalized to the 1460 cm^{-1} band [19] recorded at

Table 1
Correlation between modulation frequency and band intensities due to talc and PP (response of the 1166 and 1019 cm^{-1} bands to photothermal perturbation as a function of penetration depth)

Modulation frequency (Hz)	The 1166 cm^{-1} band correlation intensity	Approximate penetration depth (μm)	The 1019 cm^{-1} band correlation intensity
585	53 (moderate)	6.5	406 (strong)
488	16 (very weak)	7.1	337 (moderate)
195	25 (weak)	11.3	259 (moderate)
22	80 (strong)	33.6	419 (strong)

22 Hz for 2D correlation. For in-phase analysis, the spectra were first normalized and corresponding in-quadrature data were multiplied by the same normalization constant. Baseline correction was carried out on the in-phase (I) spectra. Contour levels were adjusted to illustrate the area of interest in the 22 Hz spectra and were held constant during the subsequent 2D correlations for other modulation frequencies.

3. Results and discussion

As stated above and established in the literature [20–23], SS-PA-FT-IR spectroscopy is a non-destructive method which can be used for surface depth profiling by variation of the thermal diffusion length. The origin of the PA effect is absorption of the incident infrared radiation and subsequent relaxation of vibrationally excited bands to produce thermal fluctuations in a surrounding coupling gas. As a result, thermal waves are generated [24], and the depths from which they originate is described by the following relationship:

$$\mu_s = (2\alpha/\pi f)^{1/2}$$

where μ_s is the thermal diffusion length of the sample being studied, α is the thermal diffusivity, and f is the Fourier frequency. The Fourier frequency (f) is in turn defined by the following equation:

$$f = 2V\nu$$

In this context, V is defined as the mirror velocity of the interferometer and ν is the wavenumber of the radiation for a desired band. PA data collection depends on the thermal diffusion length that is varied by the choice of the Fourier frequency (f). In a linear scan, this is accomplished by the choice of a mirror velocity. However, this approach results in a different probe depth for each wavenumber of radiation. SS-PA overcomes this limitation by serially varying modulation frequency, thereby removing the wavenumber dependence, which allows an estimate of the depth profile of the sample to be obtained [6,25].

In an effort to obtain finer depth profiling, phase rotation experiments can be employed [7–9]. This approach is similar to decomposing a vector into its x and y values, where the in-phase (0°) and in-quadrature (90°) spectra are known, and a unique vector corresponding to a phase rotation angle is obtained. Mathematical manipulations of in-phase and in-quadrature spectra will result in a spectrum represented by the following equation:

$$\Psi = I\cos\theta + Q\sin\theta$$

where Ψ is the phase rotation magnitude, I is the 0° or in-phase spectrum, Q is the 90° or in-quadrature spectrum, and θ is the phase rotation angle. Using this approach, spectra representing the area between the 0 and 90° spectra are generated, with each phase angle representing different depths. From this theoretical treatment [9], it follows that smaller phase angles will contain a greater contribution from the in-phase spectrum, and will therefore exhibit more surface character. Larger phase rotation angles will have a greater contribution from the in-quadrature spectrum and exhibit a greater bulk character. Light absorption is a function of the optical absorption coefficient (β) and this dependence results in an exponential decay in the propagation of light, which implies that the spectral areas represented by the phase-rotated spectra probably vary in a non-linear manner, with successively deeper areas representing thinner slices away from the surface as less light reaches these regions.

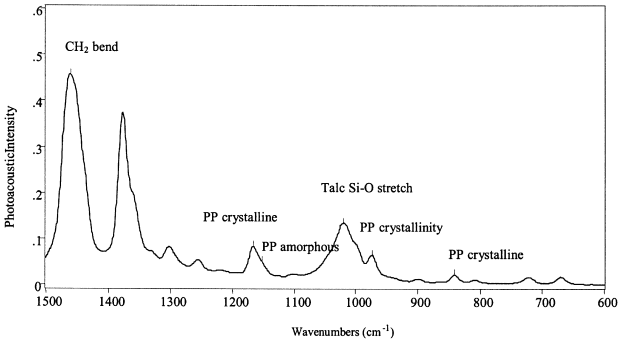

Fig. 1. Step-scan photoacoustic FT-IR spectrum of TPO recorded using 22 Hz modulation frequency.

With this background in mind, let us establish characteristic spectral features of TPOs. Fig. 1 shows a 22 Hz modulation frequency SS spectrum of TPO in the 1500–600 cm^{-1} spectral region. According to Table 1, this modulation frequency corresponds to an approximately 33.6 μm depth from the surface. As seen in Fig. 1, there are several spectral features that correspond to PP and talc, which can be used to monitor the presence of these components as a function of depth. The 1460 cm^{-1} band is attributed to the CH_2 asymmetric bending modes of bulk PP. Since this band is isolated from other vibrational modes, it can be useful for normalization purposes [18]. The band located at 973 cm^{-1} is a combination mode of molecular vibrations resulting from the CH_3 rocking and C–C chain stretching bands, and has components attributed to bulk and crystalline PP. Talc exhibits a band at 1019 cm^{-1} which is attributed to the Si–O stretching vibrations. While PP transcrystalline bands are detected at 1166 and 841 cm^{-1}, the shoulder at 1152 cm^{-1} characterizes its amorphous component [26–28].

Once component identification becomes possible, the next step is exploration of stratification among the components across the surface. Fig. 2, Trace A, shows PA-FT-IR spectrum of TPO recorded from 6.5 μm (585 Hz) and after phase rotation. At 105° phase angle, the band at 1019 cm^{-1}, which is attributed to the Si–O stretching modes of talc, is at a maximum, while the band at 844 cm^{-1}, attributed to TPO crystallinity, does not reach a maximum. As the phase rotation continues to 130° (Trace B), the band at 1019 cm^{-1} folds over onto itself, and the band at 844 cm^{-1} now reaches a maximum. The fact that the bands reach a maximum at

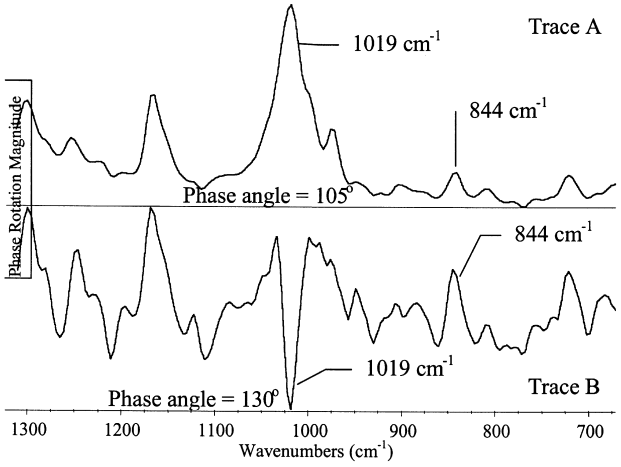

Fig. 2. Step-scan photoacoustic FT-IR spectrum of TPO recorded using 585 Hz modulation frequency. Trace A: phase angle = 105°. Trace B: phase angle = 130°.

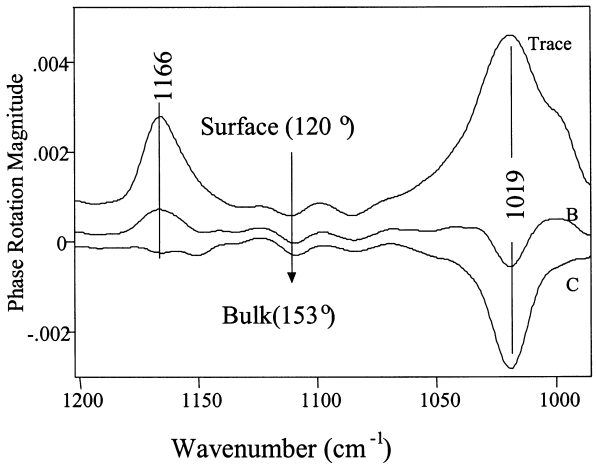

Fig. 3. Step-scan photoacoustic FT-IR spectra of TPO recorded using 585 Hz modulation frequency. Traces A–C were obtained using 120–153° phase angles.

different phase angles due to different chemical species results from photothermal phase lag [29]. As indicated earlier, signal processing in SS-PA-FT-IR is accomplished by the detection of two signals: the thermal wave that is in phase with the incident IR light and a thermal wave that was generated deeper within the thickness. Thus, heat is generated at different depths within the sample thickness and will take various amounts of time to travel to the sample surface where it can contribute to the PA signal. The result is that components from different depths within the sample will respond at different times. Since phase angle changes for signal maximization originate from phase lags of the PA signal generated from different regions in the sample, this behavior indicates that TPO stratifies. Since the 1019 cm^{-1} band folds over first, as the phase angle changes from 105 to 130°, the component responsible for this band is detected at shallower depths. Qualitative assignments of depth are possible because instrumental phase variations are cancelled out through the use of a carbon black phase reference. These results also indicate that a crystalline region of PP is further away from the surface than talc.

Since characterization by a single modulation frequency only provides partial stratification information, other modulation frequencies will be examined. Fig. 3 shows in-phase and in-quadrature spectra of a TPO sample in the 1200–1000 cm^{-1} region. These spectra were collected in a SS mode at a depth of 6.5 μm (585 Hz). At 120° phase angle (Trace A) the band at 1019 cm^{-1} and the band at 1166 cm^{-1} due to TPO crystallinity are pointing upwards. At 135° phase angle (Trace B), the band at 1019 cm^{-1} folds over onto itself while the band at 1166 cm^{-1} is still pointing upwards. As rotation continues to 150° (Trace C), both bands eventually become negative. These results confirm the data discussed in Fig. 2 and also indicate that the talc and PP components stratify. The choice of 585 Hz modulation frequency was dictated by the fact that this frequency provides an approximately 6.5 μm depth of penetration and initial analysis showed a lag in the PA phase between components at this modulation frequency.

Since the phase rotation analysis provides information about stratification of the TPO components, a 2D correlation analysis of SS-PA-FT-IR spectra at several modulation frequencies will be employed allowing a measurement of phase and magnitude properties at the same time. In this case, perturbation is accomplished by utilization of the photothermal effect, in which sinusoidally modulated IR light is absorbed, followed by conversion into thermal energy propagating in a sinusoidal manner. As a result of heat evolution, internal perturbation occurs that results from thermal waves propagating through the specimen. Thermal diffusion length, μ_{th}, that is a distance from which thermal waves can reach the surface, is controlled by choosing the modulation frequency [19,20]. Using this perturbation it is possible to establish the time dependence of the PA signal, which ultimately will allow us to determine which particular chemical functional groups or species are present at a particular depth from the sample surface.

In an effort to obtain spectral information from various depths, 585, 488, 195, and 22 Hz modulation frequencies were chosen. These modulation frequencies correspond to approximate penetration depths of 6.5, 7.1, 11.3, and 33.6 μm, respectively. Following 2D FT-IR principles [10–13], analysis of auto-peaks, spectral features occurring on the diagonal of synchronous correlation diagrams, represent species that respond in-phase with the perturbation. In this case the perturbation is the photothermal effect which provides depth information due to thermal phase lags with respect to input IR radiation. Auto-correlation at a given modulation frequency indicates that both surface and bulk signals act in a coherent manner. If correlation intensity is present for a given wavenumber in the auto-peak position, the chemical species or functional groups are present at that depth. Furthermore, an increase in auto-correlation bands when comparing data from different modulation frequencies

indicates a relative increase of concentration level for the species exhibiting the increase in correlation intensity. The results of synchronous 2D-correlation analysis performed on TPO at various probe depths are shown in Fig. 4a–d.

According to the synchronous correlation diagrams shown in Fig. 4a–d, a PA intensity column was added to Table 1 which illustrates the results of 2D FT-IR synchronous correlation analysis, for which the bands at 1019 and 1166 cm^{-1} were used. As we recall, these bands are the Si–O vibrations in talc and transcrystalline PP, respectively. Table 1 shows how auto-correlation intensity changes occur with respect to modulation frequency. Based on the correlation intensity data it can be seen that PP exhibits less intensity than talc at all levels, which is the result of different extinction coefficients for the two bands. As a result, the contour levels must be adjusted to focus on the area of interest when examining multiple components. It should be kept in mind that the data is intact, only the point at which slices are made through the data is being changed. At 6.5 μm from the surface (Fig. 4a), the band due to PP crystallinity exhibits moderate intensity relative to the correlation intensities obtained from other depths. At 7.1 μm (Fig. 4b) the correlation intensity due to the PP crystallinity vanishes, indicating that this species is no longer present at the probed depth. As perturbation depth increases further to 11.3 μm (Fig. 4c), a trace of PP crystallinity is detected as indicated by weak correlation intensity appearing again on the diagonal. At 33.6 μm (Fig. 4d), there is strong correlation intensity due to both species, indicating that PP and talc exist in greater amounts at this depth than the preceding probed depth.

Using these data the stratification diagram shown in Fig. 5

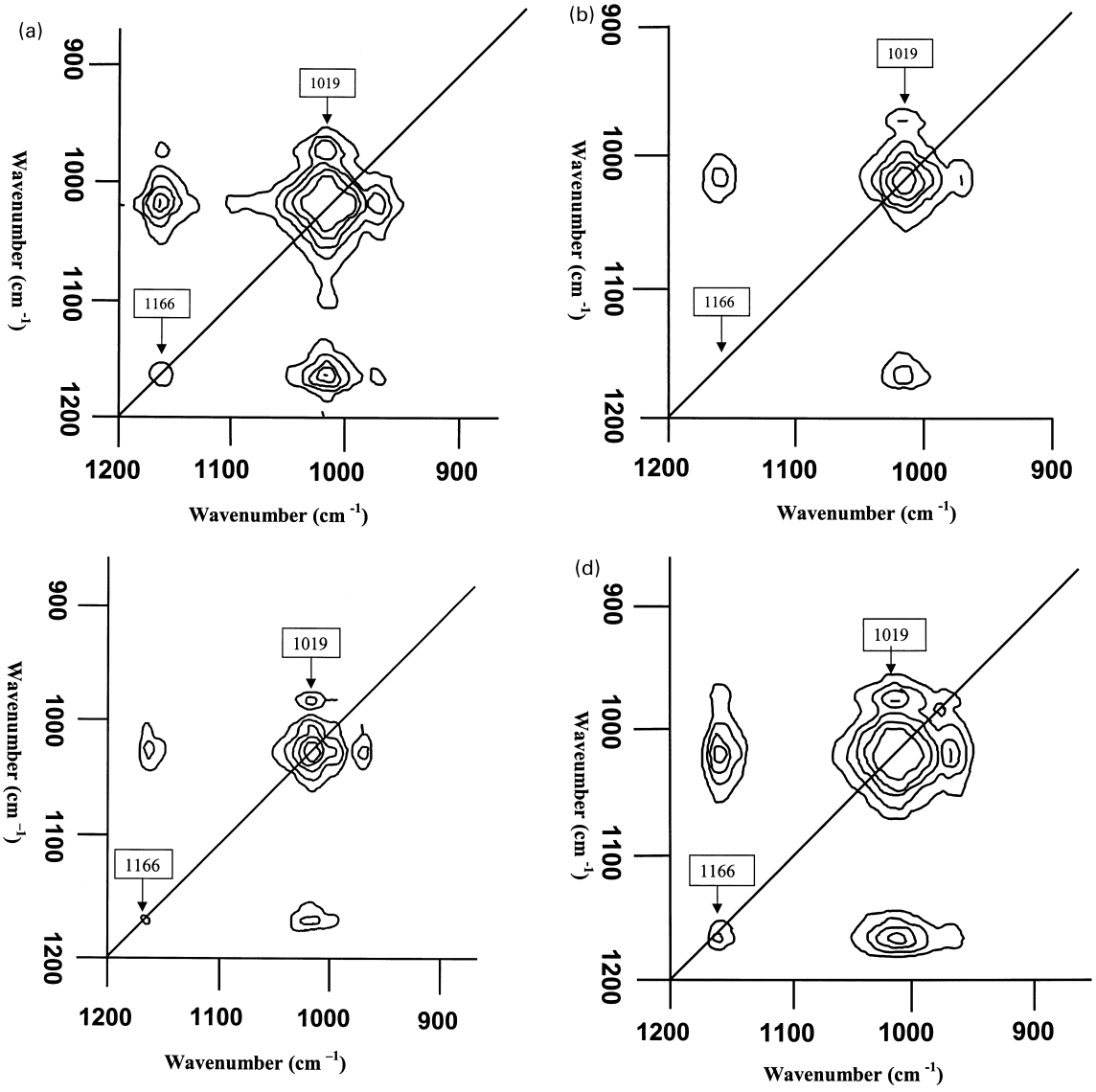

Fig. 4. 2D synchronous correlation step-scan FT-IR spectrum recorded at (a) 585 Hz, (b) 488 Hz, (c) 195 Hz, and (d) 22 Hz of TPO in the range of talc absorption.

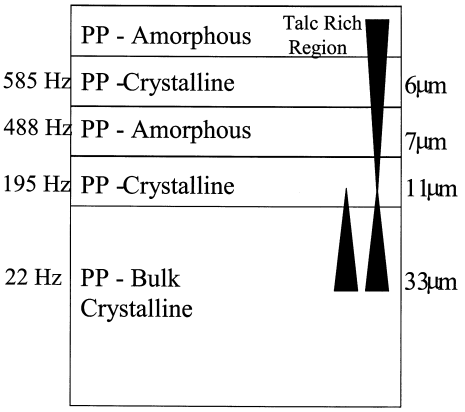

Fig. 5. Stratification of talc and PP in TPO surface.

was constructed with respect to the distribution of PP crystallinity in TPO. In order to examine talc concentration changes, contour levels that more closely approach the talc maximum correlation intensity are chosen. As seen at 6.5 μm (Fig. 4a) from the surface, the band due to talc exhibits strong correlation intensity, but at 7.1 μm (Fig. 4b) the correlation intensity decreases. As perturbation depth increases further to 11.3 μm (Fig. 4c), the talc correlation intensity remains moderate and at 33.6 μm (Fig. 4d) becomes strong due to the presence of talc at this depth.

4. Conclusions

These studies show that the use of an internal perturbation caused by the photothermal effect allows enhancement of the PA response from various surface depths. The combined use of phase and 2D correlation analyses allowed us to determine that individual components of TPO stratify as a result of thermal history and processing. It was found that there are talc rich regions near the surface (6.5 μm) of the TPO along with transcrystalline PP. At depths ranging from 7.1 to 11.3 μm, talc content as well as PP transcrystalline phase decrease. As the sample is probed at 33.6 μm, another talc rich region becomes apparent and bulk PP shows a large increase in crystallinity. Earlier in the paper it was noted that these areas rich in PP crystalline phase and talc are expected to have a decreased concentration of elastomer and PP amorphous phase. As noted in the introduction, such surface stratification processes in TPO might have a very significant influence on adhesion of organic films to TPO.

Acknowledgements

The authors are thankful to the National Science Foundation Industry/University Cooperative Research Center in Coatings at the University of Southern Mississippi and Eastern Michigan University for support of these studies.

References

[1] Prater TJ, Kaberline SL, Holubka JW, Ryntz RA. J Coat Technol 1996;68:83.
[2] Ryntz RA. Prog Org Coat 1996;27:241.
[3] Fitchmun DR, Mencik Z. J Polym Sci, Polym Phys Ed 1973;11:951.
[4] Pennington BD, Ryntz RM, Urban MW. Polymer 1999;40:4795.
[5] Niu B-J, Urban MW. J Appl Polym Sci 1998;70:1321.
[6] Dittmar RM, Chao JL, Palmer RA. Springer series in optical sciences: photoacoustic and photothermal phenomena III, vol. 6. Berlin: Springer, 1992 (p. 492).
[7] Drapcho DC, Curbelok R, Jiang EY, Crocombe RA, McCarthy WJ. Appl Spectrosc 1997;51:453.
[8] Palmer RA, Jiang EY. J Phys, IV 1994;4:c7–337 (Colloq C7, supplement au J Phys III).
[9] Jones RW, McClelland JF. Appl Spectrosc 1996;50:1258.
[10] Noda I. Appl Spectrosc 1990;44:550.
[11] Noda I. Appl Spectrosc 1993;47:1329.
[12] Noda I, Dowrey DA, Marcott C. Appl Spectrosc 1993;47:1317.
[13] Noda IF. Am Chem Soc 1989;111:8116.
[14] Sonoyama M, Shoda K, Katagiri G, Ishida H. Appl Spectrosc 1996;50:377.
[15] Story GM, Marcott C, Noda E. SPIE Proc 1993;2089.
[16] Marcott C, Story GM, Noda I. Abstracts of the Pittsburgh Conference on Analytical and Applied Spectroscopy. New Orleans, LA, Paper #1043, 1995.
[17] Jiang EY, Palmer RA, Barr NE, Morosoff N. Appl Spectrosc 1997;51:1238.
[18] Chen G, Fina LJ. J Appl Polym Sci 1993;48:1229.
[19] Urban MW, Gaboury SR, McDonald WF, Tiefenthaler AM. Polymer characterization; physical property, spectroscopic, and chromatogaphic methods, Advances in Chemistry Series #227. Washington, DC: American Chemical Society, 1990.
[20] Urban MW, Koenig JL. Appl Spectrosc 1986;40:994.
[21] Urban MW. J Coat Technol 1987;59:29.
[22] Choquet M, Rousset G, Bertrand L. Can J Phys 1985;64:1081.
[23] Bertrand L. Appl Spectrosc 1988;42:134.
[24] Graham JA, Grim III WM, Fateley WG. In: Ferraro JR, Basile LJ, editors. Fourier transform infrared spectroscopy, vol. 4. New York: Academic Press, 1985. p. 345.
[25] Palmer RA, Chao JL, Dittmar RM, Gregoriou VG, Plunkett SE. Appl Spectrosc 1993;47:1297.
[26] Tadokoro H, Kobayashi M, Ukita M, Yasufuku K, Shunsuke M, Torii T. J Chem Phys 1965;42:1432.
[27] Painter PC, Watzek M, Koenig JL. Polymer 1977;18:1172.
[28] Natta G, Pino P, Corradini P, Danusso F, Mantica E, Mazzanti G, Moraglio G. J Am Chem Soc 1955;77:1710.
[29] Jiang EY, Palmer RA, Chao JL. J Appl Phys 1995;78:460.